Plasmon Enhanced Terahertz Emission from Single Layer Graphene

Young-Mi Bahk,[†,#] Gopakumar Ramakrishnan,[‡,▽,#] Jongho Choi,[§] Hyelynn Song,[§] Geunchang Choi,[†] Yong Hyup Kim,[§,⊥] Kwang Jun Ahn,[∥] Dai-Sik Kim,[†,*] and Paul C. M. Planken[‡,*]

[†]Center for Subwavelength Optics and Department of Physics and Astronomy, Seoul National University, Seoul 151-747, Korea, [‡]Optics Research Group, Department of Imaging Physics, Faculty of Applied Sciences, Delft University of Technology, Lorentzweg 1, 2628 CJ Delft, The Netherlands, [§]School of Mechanical and Aerospace Engineering, Seoul National University, Seoul 151-742, Korea, [⊥]Institute of Advanced Aerospace Technology, Seoul National University, 1 Gwanak-gu, Seoul 151-742, Korea, and [∥]Department of Energy Systems Research and Department of Physics, Ajou University, Suwon-si 443-749, Korea. [#]These authors contributed equally to this work. [▽]Present address: School of Chemistry and WestCHEM, University of Glasgow, Glasgow, G12 8QQ, United Kingdom.

ABSTRACT We show that surface plasmons, excited with femtosecond laser pulses on continuous or discontinuous gold substrates, strongly enhance the generation and emission of ultrashort, broadband terahertz pulses from single layer graphene. Without surface plasmon excitation, for graphene on glass, '*nonresonant laser-pulse-induced photon drag currents*' appear to be responsible for the relatively weak emission of both *s*- and *p*-polarized terahertz pulses. For graphene on a discontinuous layer of gold, only the emission of the *p*-polarized terahertz electric field is enhanced, whereas the *s*-polarized component remains largely unaffected, suggesting the presence of an additional terahertz generation mechanism. We argue that in the latter case, '*surface-plasmon-enhanced optical rectification*', made possible by the lack of inversion symmetry at the graphene on gold surface, is responsible for the strongly enhanced emission. The enhancement occurs because the electric field of surface plasmons is localized and enhanced where the graphene is located: at the surface of the metal. We believe that our results point the way to small, thin, and more efficient terahertz photonic devices.

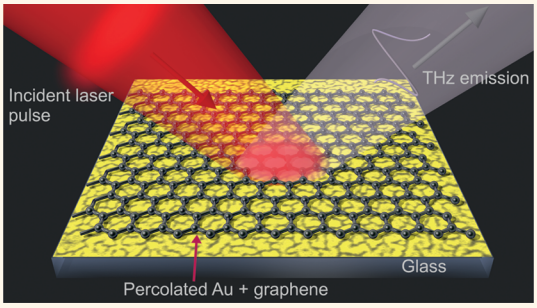

KEYWORDS: terahertz spectroscopy · surface plasmon · ultrafast photon drag · graphene · gold nanostructures

Graphene, a two-dimensional monolayer of carbon atoms, is a zero band gap semiconductor.[1−5] Because of its potential use in ultrahigh speed photonic devices, there has been an increased interest in the optical properties of graphene. Nonlinear optical properties of graphene, such as second[6−9] and third harmonic generation,[10] frequency mixing,[11] photon drag effect,[12−16] optical Kerr effect,[17] and excitation of photocurrents,[18,19] have been extensively studied both experimentally and theoretically. The effects observed are strongly enhanced compared with those in conventional semiconductors because of the extraordinary electrical and optical properties caused by the high electron mobility and linear dispersion in graphene. Recently, diverse graphene-based optoelectronic devices making use of the optical nonlinearities and the ultrafast carrier dynamics have been demonstrated or proposed.[20,21]

The remarkable properties of graphene have also led to a growing interest in the possible use of this material as a source/detector of terahertz (THz) radiation.[18,19,22−25] THz generation through ultrafast nonlinear optical phenomena has been reported in graphite-related materials.[16,18,19,25−31] However, one of the major hurdles for using graphene as a source of THz radiation in such cases is its small interaction with light, owing to the single atom thickness.

There have been different attempts to generate THz radiation from graphene. In 2012, Boubanga-Tombet *et al.* reported the amplification of incoming THz light by optically pumped exfoliated graphene.[25] The excitation of ultrafast laser-generated picosecond photocurrents in freely suspended graphene was shown by Prechtel *et al.*[19] Very recently, results were reported by Obraztsov *et al.* showing that photon-drag currents, *i.e.*, the currents induced by the momentum transfer from photons to

* Address correspondence to dsk@phya.snu.ac.kr, p.c.m.planken@tudelft.nl.

Received for review May 8, 2014 and accepted August 19, 2014.

Published online August 19, 2014
10.1021/nn5025237

© 2014 American Chemical Society

electrons, give rise to the emission of THz pulses by graphene.[16]

In this report, we confirm the observation of broadband THz emission from a single layer of graphene, excited by femtosecond near-infrared laser pulses and show how the excitation of surface plasmons strongly enhances the emission. Our results show that for graphene deposited on a glass substrate, the amplitude of the emitted THz electric field strongly varies and even reverses sign when the pump-beam polarization direction is changed. This behavior is consistent with the model of '*nonresonant photon drag effect*' (NDE),[12] which is the excitation of photocurrents by photon-electron momentum transfer, as the source of the THz emission. For graphene deposited on thin gold (Au) films, however, the emitted THz power is significantly enhanced by 2 orders of magnitude when propagating and localized surface plasmons are excited. In particular, from the results of graphene on a discontinuous Au layer, we argue that an additional generation mechanism, '*optical rectification*' resulting from a strong lack of inversion symmetry of graphene on the Au substrate, begins to dominate the emission of the *p*-polarized THz light. The emission of *s*-polarized THz light, most likely caused by the nonresonant excitation of photon drag currents, seems to be unaffected by the localized surface plasmon excitation.

RESULTS AND DISCUSSION

The graphene layers are directly synthesized by a chemical vapor deposition (CVD) system and transferred onto a glass slide and a thin Au film on a glass substrate (see Figure 1a). In Figure 1b, we show a Raman spectrum of the graphene sample using excitation at a wavelength of 532 nm. The intensity ratio of the 2D peak (~2680 cm^{-1}) with respect to the G peak (~1590 cm^{-1}) is ~3. Note that the D band (expected near 1350 cm^{-1}) is absent, indicating a high purity of the graphene layers with a low number of defects.

As illustrated in Figure 1c,d, the experiments were performed using a standard THz time-domain spectroscopy setup based on electro-optic sampling using a 0.5 mm thick (110) oriented zinc telluride (ZnTe) crystal.[32,33] Graphene prepared on a transparent glass substrate is excited with the pump light in two different ways, depending on the experiment. In one case, the pump beam excites the graphene from the back side through the glass substrate as shown in Figure 1c. The emitted THz light is collected in the transmission direction of the pump light. The graphene layer can also be excited in a reflection type setup as shown in Figure 1d, in which the pump light illuminates the sample on the graphene layer side, and the generated THz light is collected in the reflection direction of the pump light.

Typical time traces of the detected THz electric field, emitted from a single layer graphene on glass,

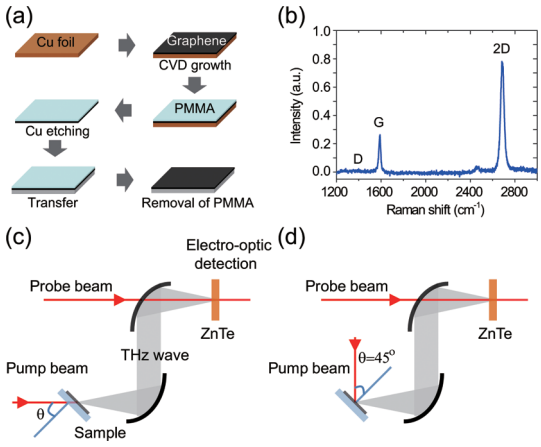

Figure 1. (a) Synthesis, etching, and transfer processes for a single layer graphene film. (b) Raman spectrum of the sample showing G and 2D modes of single layer graphene (laser excitation at 532 nm). Note that the D band is absent. (c and d) Schematics of transmission (c) and reflection types (d) of THz generation setups.

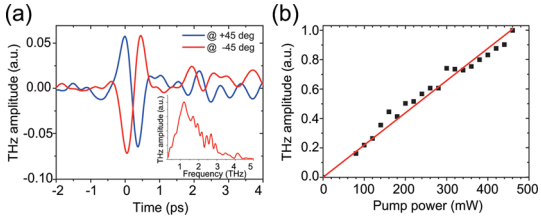

Figure 2. (a) Typical time traces of the emitted THz electric field from the single layer graphene on a glass slide, measured in the transmission type setup. The incident angles of the pump beam are +45° (blue) and −45° (red). Note that no emission is detected for 0°. Inset: Fourier-transformed THz electric-field amplitude as a function of frequency. (b) Emitted THz amplitude from the graphene sample on a glass substrate *vs* incident pump power.

are measured in a transmission setup as shown in Figure 2a. The pulses have a subpicosecond duration and consist of a nearly single cycle oscillation followed by a weaker and rapidly oscillating trace which is the result of absorption and re-emission of the THz light by water molecules in the atmosphere. The inset of the figure shows the spectrum of the emitted THz electric-field amplitude obtained by Fourier-transformation. The frequency of the maximum THz amplitude is about 1.2 THz. The measured electric field from which the broad spectrum was calculated was obtained in ambient atmosphere. In Figure 2b, we plot the measured THz amplitude as a function of incident laser power. The figure shows that the amplitude increases linearly with laser power, suggesting that a second order nonlinear optical process is responsible for the emission. As shown in Figure 2a, when the incident angle of the pump beam θ is changed from +45° to −45°, the polarity of the emitted THz pulse is reversed. No THz emission is detected at normal incidence of the pump beam (θ = 0°). The emitted THz amplitude is thus an odd function of the incident angle. In general for a

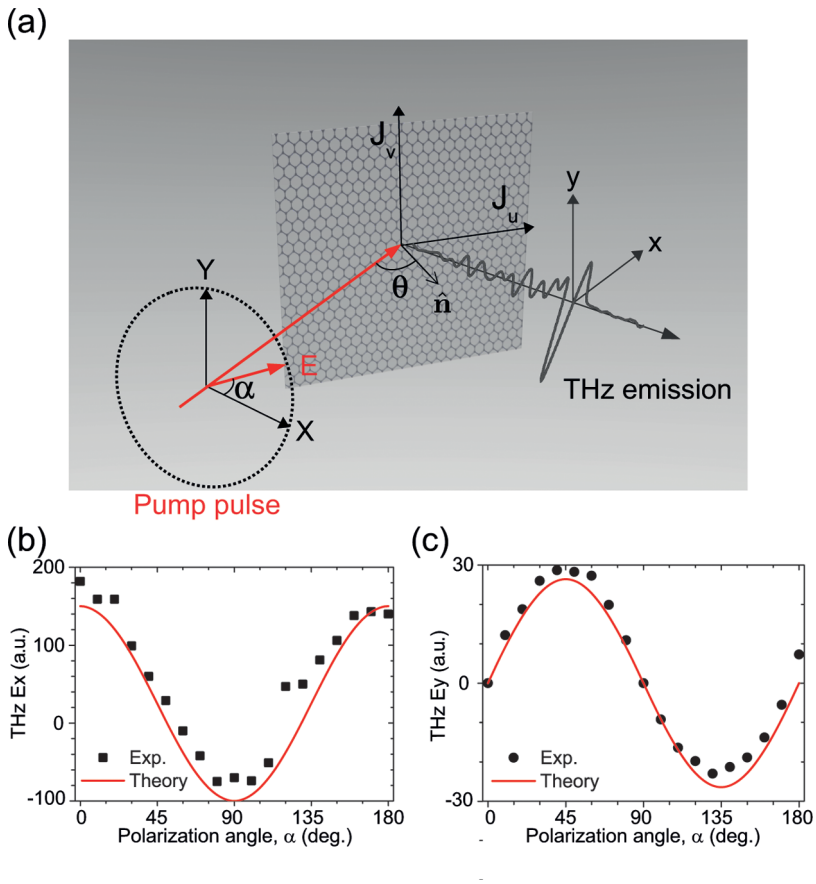

Figure 3. (a) Schematic of the excitation of single layer graphene for polarization dependence experiment. (b and c) *x*- (b) and *y*-components (c) of generated THz amplitudes depending on the incident polarization angle α when $\theta = 45°$.

conventional THz emitter material such as gallium arsenide (GaAs), such a sign change is evidence of photoinduced currents propagating in a direction perpendicular to the surface.[34] Since such currents are obviously not possible in graphene because it is only a single atomic layer, the emission might be due to *nonresonant* optical rectification by a non-zero electric susceptibility $\chi^{(2)}$, requiring the absence of a center of inversion symmetry. An ideal graphene layer possesses an in-plane center of inversion symmetry. Nonresonant optical rectification is only possible along the surface normal where the inversion symmetry is broken, because the graphene sample is deposited on glass substrates. The asymmetry along the surface normal can, however, be removed by sandwiching graphene in between two layers of the same material. Therefore, the graphene layer was prepared in between two 24 nm thick aluminum oxide (Al_2O_3) layers on a glass substrate. However, no significant change in the THz emission was observed from the sandwiched graphene layer, as compared to the bare graphene layers on glass, making the case of surface nonlinearity as the source of the emission unlikely.

The THz emission from single layer graphene must therefore be taking place through a different mechanism. To shed more light on the emission mechanism, we varied the polarization of the pump beam using a half-wave plate as shown schematically in Figure 3a. The incident angle θ is fixed at 45°. The polarization angle α of the pump beam is defined as the azimuthal rotation of the polarization angle from the *p*-polarization state. In Figure 3b, we plot the *x*-component of the generated THz electric field as a function of the polarization state of the incident pump light. The *x*-component of the THz electric field shows a change of polarity when α is rotated by an angle of ~60°. The sign reversal is observed again, as the rotation angle of α reaches ~120°. In Figure 3c, we plot the *y*-component of the detected THz pulse. Again we emphasize that standard semiconductor THz emitters based on transient photocurrents perpendicular to the surface do not emit such an *s*-polarized THz electric field. Interestingly, the *y*-component of the THz electric field appears only when both *p*- and *s*-polarization components of the pump beam are simultaneously present. As the polarization of the pump beam is rotated by more than 90°, the *y*-component of the THz electric field also changes polarity. This polarization dependence cannot be explained by surface related nonlinear optical effects. At this point, based on these experimental results, we can conclude that the mechanism of THz emission from single layer graphene seems to be different from

those already reported in the literature,[18,19,25−31] but our results quite resemble a recent report suggesting that "photon drag current" might be the cause of the THz emission.[16]

Despite the large number of reports on photon drag effects in the literature, little is known about their contribution to the THz emission through the optical excitation of ultrafast laser pulses in semiconductors or on metal surfaces. NDE is the result of the momentum transfer from pump photons to the electrons in the material. As a result, the electrons are "dragged" along with the propagation direction of photons and a *dc* photocurrent develops in the material. Similarly, the photogalvanic effect also leads to the generation of a *dc* photocurrent in the material. However, in such cases the spatial inversion symmetry needs to be broken. In single layer graphene, photon drag and photogalvanic effects have been theoretically well investigated.[12] These effects arise from the unique ballistic or quasi-ballistic electron transport properties of graphene and related materials.[12−15,35−37]

Our experiments are performed within the condition of NDE: $|\omega - 2\varepsilon_F| > sq$, where ω is frequency of photon, ε_F is Fermi energy, s is the electron velocity, and q is the projection of the photon wave-vector to the sample plane. The components of the drag current j_u and j_v in the plane of the graphene layer depend on the polarization of the pump beam as follows,

$$j_u \propto \frac{3}{2}\cos^2\alpha - \sin^2\alpha$$

and

$$j_v \propto \cos\alpha \sin\alpha$$

With $E_{THz,x} \propto (\partial j_u/\partial t)$ and $E_{THz,y} \propto (\partial j_v/\partial t)$, we can similarly write the THz electric field components depending on the polarization as

$$E_{THz,x} \propto \frac{3}{2}\cos^2\alpha - \sin^2\alpha$$

and

$$E_{THz,y} \propto \cos\alpha \sin\alpha$$

which are valid for a 45° angle of incidence. In Figure 3b,c, we plot these expressions with the measured results, where we vertically scaled the expressions to obtain the best fit. On the basis of the excellent fit of the calculated values to the experimental data, and in accordance with recent reports,[12,16] it is likely that the physical mechanism of THz emission from an unbiased single layer graphene on a glass substrate is mainly the excitation of ultrafast photocurrents through the photon drag effect. Note that, as the duration of the emitted THz pulse is <1 ps, it must result from the electron transport over short propagation distances <1 μm. Thus, the emitted THz pulse can be used as a probe to study the local electron transport in graphene without requiring the application of electrical contacts.

The THz emission from single layer graphene is fairly weak. In our setup, the peak value of THz amplitude from graphene on glass is ∼10 mV/cm with a THz pulse energy of $\sim 10^{-20}$ J (Supporting Information). To enhance the THz emission, surface plasmon resonance excitation at graphene/metal interfaces can be used.[38−45] Very recently, Ramakrishnan *et al.* reported the plasmonic enhancement of THz emission from ultrathin semiconductor films deposited on Au surfaces.[46] The assumption is that at a metal surface, the plasmon pump field is enhanced compared to the field of a conventional propagating wave incident on the metal, enhancing nonlinear processes occurring at or near the metal surface. In what follows, we illustrate this by using both *propagating* as well as *localized* surface plasmons at a graphene/metal interface.

In the first experiment, we used the so-called Kretschmann geometry to excite surface plasmons on a flat Au surface (Figure 4a). A Au film of 44 nm thickness is deposited on the hypotenuse side of a right-angle prism, using electron-beam evaporation under high vacuum conditions (below a pressure of 10^{-6} mbar).[47] The single layer graphene is transferred onto the Au film. The pump beam enters from the glass side. In Figure 4b, the reflected pump power from the prism with and without the graphene layer is shown as a function of the incident angle of the pump beam. When the incident angle is ∼45°, the reflected pump power from the prism reaches a minimum. This significant reduction of the reflection intensity comes from the resonant coupling of the evanescent wave field to propagating surface plasmon modes. This incident angle is called the surface plasmon resonance (SPR) angle, which is sensitive to the surface conditions of the Au layer: the SPR angle shifts from 44.60° (without graphene) to 44.84° (with graphene).[40]

In Figure 4c, we plot the peak value of the generated THz electric field and the reflected pump power from the prism with graphene as a function of the incident angle θ. We observe that the emitted THz amplitude is significantly enhanced when surface plasmons are resonantly excited at the Au surface/graphene interface. The enhancement factor is ∼30 (power enhancement of ∼900) compared to the THz amplitude emitted by the graphene on the glass. The enhancement occurs due to the increased interaction of the pump light with graphene *via* the strongly localized and enhanced electric field of the surface plasmons excited near the Au surface. We note that the SPR angle and the maximum of the emitted THz amplitude are separated by ∼0.2°. This shift can be accounted for the surface plasmon hybridization, where the bound and leaky symmetric modes are generated when the metal film becomes thin and lossy. Only the leaky mode contributes to the intensity localization on the

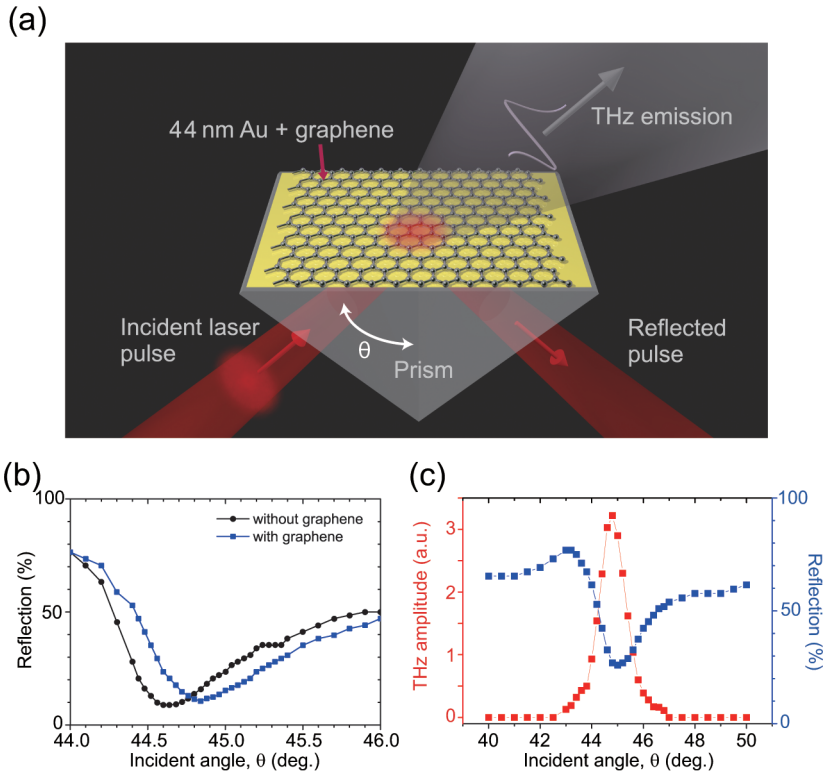

Figure 4. (a) The Kretschmann geometry used for the excitation of the single layer graphene on a Au film. θ is the angle of incidence for the pump beam measured outside the prism. (b) Reflected pump power as a function of the incident angle θ for 44 nm thick Au film on prism with graphene layer (blue) and without graphene layer (black). (c) THz electric field amplitude (red) from the single layer graphene on the Au film and reflected pump power (blue), plotted as functions of the incident angle θ.

graphene layer.[48] In this experiment, we cannot excite graphene with *s*-polarized light because surface plasmons can be excited only with a *p*-polarized pump beam. Accordingly, it is not possible to see the effects of the polarization dependence.

In the second experiment, we increased the local pump intensity by the excitation of localized surface plasmons on a semicontinuous percolating Au film. When Au films are prepared by physical vapor deposition on substrates like glass, the morphology of the film is changed from randomly placed isolated nanoislands to a percolated state as the average thickness of the metal layer increases to ~7 nm. The ultrathin semicontinuous Au films near the percolation threshold have been shown to enhance the nonlinear optical properties of the metal, and of a second material placed on top due to the hot spots of localized surface plasmons. THz generation by illuminating percolating Au films on glass substrates with femtosecond laser pulses was reported earlier by Ramakrishnan and Planken in 2011.[49] In the present experiment, we used the strong field enhancement of a percolating film to increase the THz emission from a single layer of graphene. We prepared an Au film of ~10 nm *average-thickness* on a glass slide by electron-beam evaporation and transferred a single layer graphene to the Au film (Figure 5a). In Figure 5b, a scanning electron microscope (SEM) image of graphene on the percolating Au film is shown. Figure 5c shows the atomic force microscope (AFM) images of an Au film of 10 nm average thickness deposited on a glass slide without graphene layer (left) and with graphene layer (right), scanned at different positions. The graphene layer does not seem to follow the morphology of the percolating gold layer. The experiments are performed in a reflection-type setup. Figure 5d shows the THz electric field emitted from a single layer graphene on a percolating Au film (red), a single layer graphene on glass (blue) and from a percolating Au film (black). Considering the possible variation of the THz amplitude for different positions on the sample, we find that the THz power emitted from graphene on the Au film is significantly enhanced by a factor of ~81 with respect to that from graphene on glass (Figure S1 (Supporting Information)). This indicates that the strongly localized surface plasmons of the percolating Au film play a major role in enhancing the THz emission. In Figure 5e, we plot the measured THz amplitude as a function of the pump power. The amplitude clearly increases linearly, indicating that the emission is still a second-order nonlinear optical process.

To understand the mechanism behind the enhanced emission of THz light by graphene on percolating Au, we plot in Figure 6 the emitted THz amplitude as a

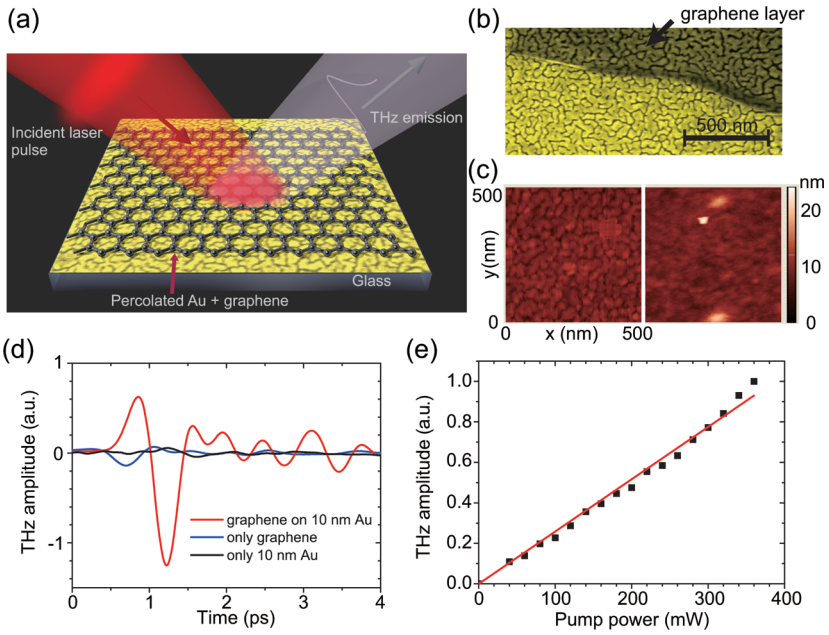

Figure 5. (a) The excitation of graphene deposited on percolating Au layer. (b) A pseudocolor SEM image of a single layer graphene on a Au film of 10 nm average thickness deposited on a glass substrate. The Au layer shows a randomly shaped nanostructure at this thickness. (c) AFM images of an Au film of 10 nm average thickness deposited on a glass without graphene layer (left) and with graphene layer (right), scanned at different positions. (d) THz electric field pulse as a function of time, emitted from a single layer graphene on a percolating Au film of 10 nm average thickness (red), only graphene (blue), and only percolated Au film (black). (e) THz amplitude emitted from a single layer graphene on the percolated Au film, plotted as a function of the incident pump power.

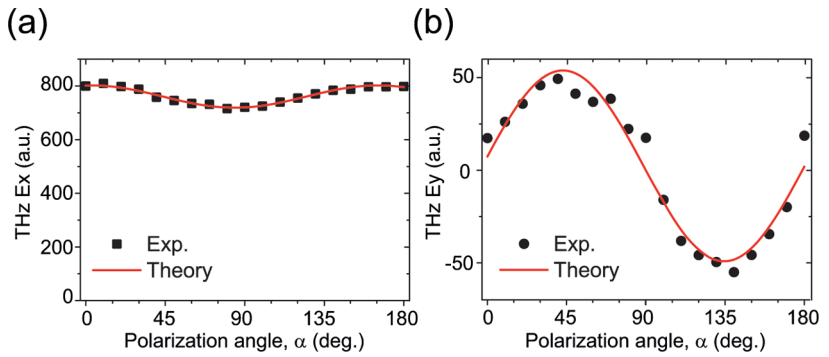

Figure 6. (a) *x*- and (b) *y*-components of THz amplitude emitted from a single layer of graphene on a 10 nm thick Au layer, plotted against the incident pump polarization angle α. The angle of incidence $\theta = 45°$. The dotted lines are the measurement data and the solid lines are the mathematical fits.

function of the polarization angle of the incident beam. The *x*-component of the THz electric field (Figure 6a) shows a weak *cosine* dependence on the pump polarization angle with a large pump-polarization-independent constant contribution. Excitation with *p*-polarized pump light ($\alpha = 0°$ and 180°) results in slightly stronger THz emission than with *s*-polarized ($\alpha = 90°$) light. In contrast in Figure 6b, we see that the *y*-component of the emitted THz electric field shows a similar behavior as seen earlier in Figure 3c, in the case of single layer graphene on a glass substrate. One interesting thing is that a remarkable enhancement is only observed for the *x*-component of the THz electric field (Figure 6a), compared to the results from a single layer graphene on a glass substrate (Figure 3b), whereas no significant change is observed for the *y*-component (Figure 6b). These results suggest that the specific enhancement observed for the *x*-component emission may be due to an additional source term. In a direction perpendicular to the surface, the inversion symmetry is broken due to the presence of the Au layer, giving rise to an additional second-order optical nonlinearity. Using this additional nonlinearity, the excitation of "hot spots" of localized surface plasmon can contribute to the enhancement of the optical rectification of the pump laser pulses. In ref 49, it has been shown that such a surface nonlinearity only gives rise to *p*-polarized THz emission, explaining why no enhancement is observed for the emitted *s*-polarized THz electric field component.[49] We emphasize that for the enhancement, both the percolating Au

and the graphene need to be present. Either graphene (on glass) or percolating Au emits THz pulses with 1 order of magnitude smaller amplitude. The emitted THz amplitude from single layer graphene on 10 nm thick Au layer is about 4% of the THz amplitude emitted from an unbiased (100) oriented semi-insulating GaAs surface, surprisingly strong, considering the single atomic layer thickness of graphene.

CONCLUSIONS

We report the emission of broadband THz radiation when single layer graphene is illuminated with femtosecond near-infrared laser pulses. Our experimental results indicate that for graphene on glass, the emission is most likely through the excitation of ultrafast transient photon drag currents, thus fulfilling the promise of a Dirac material for the giant photon drag effect at modest peak powers. We demonstrate that a strong enhancement in the emission can be achieved by excitation of strongly localized as well as propagating surface plasmons in the vicinity of graphene. The localized surface plasmon excitation on randomly nanostructured Au films is seen to particularly enhance the THz emission through enhanced optical rectification through the surface $\chi^{(2)}$ of the layer, which is not observed in the case of graphene on a glass substrate. Our work points toward the possibility of developing graphene-based ultrafast THz photonic devices.

METHODS

Sample Fabrication. The graphene layers are directly synthesized on copper (Cu) foils by chemical vapor deposition (CVD), after which a poly(methyl methacrylate) (PMMA) film was spin-coated for the transfer (see Figure 1a). The Cu substrates are then dissolved in a 0.1 M ammonium persulfate ($(NH_4)_2S_2O_8$) solution. The floating graphene/PMMA films are subsequently transferred onto a glass slide and a thin Au film on a glass substrate, and the PMMA film is finally removed by chloroform.

Experimental Method. A standard THz time-domain spectroscopy setup is used for the experiments. The samples are illuminated with the output from a laser source, a Ti:sapphire oscillator (Femtosource XL) generating *p*-polarized light pulses centered at a wavelength of 800 nm with 50 fs duration and 11 MHz repetition rate. The average output power from the laser is ~800 mW. About 80% of the laser energy is used as the pump beam for exciting the samples, and the remaining ~20% is used as the probe beam for detecting the emitted THz light. The pump beam is focused to a spot size of ~2 mm on the sample. The emitted THz light is collected and guided to the detection setup using two paraboloidal mirrors. The amplitude of the emitted THz light electric field is detected by free-space electro-optic sampling method with a 0.5 mm thick (110) oriented zinc telluride (ZnTe) crystal.

Conflict of Interest: The authors declare no competing financial interest.

Acknowledgment. This work was supported by the National Research Foundation of Korea (NRF) grant funded by the Korea government (MSIP) (No. 2008-0061906, 2005-0093838, 2008-00580) (No. 2009-0083512, 2014R1A2A1A05007760). This work was also supported by the Brain Korea 21 Plus Project in 2014. P.C.M.P. thanks the Nederlandse Organisatie voor Wetenschappelijk Onderzoek (NWO) and the Stichting voor Technische Wetenschappen (STW) for the financial support in the form of a 'VICI' grant. The financial support from NanoNextNL is also gratefully acknowledged. We thank Sung Ju Hong (SNU) for the measurement of graphene properties, and Nishant Kumar (TU Delft) for the GaAs terahertz emission measurement.

Supporting Information Available: Details of how each THz measurement was carried out; comparison of the THz amplitudes emitted from different arbitrary positions on only graphene on glass and graphene on percolating Au on glass (Figure S1); estimation of the carrier mobility of graphene samples used in the study, (Figure S2) and calculation of the absolute value of the THz electric field and the THz pulse energy emitted from only graphene on glass. This material is available free of charge *via* the Internet at http://pubs.acs.org.

REFERENCES AND NOTES

1. Novoselov, K. S.; Geim, A. K.; Morozov, S. V.; Jiang, D.; Zhang, Y.; Dubonos, S. V.; Grigorieva, I. V.; Firsov, A. A. Electric Field Effect in Atomically Thin Carbon Films. *Science* **2004**, *306*, 666–669.
2. Novoselov, K. S.; Geim, A. K.; Morozov, S. V.; Jiang, D.; Katsnelson, M. I.; Grigorieva, I. V.; Dubonos, S. V.; Firsov, A. A. Two-Dimensional Gas of Massless Dirac Fermions in Graphene. *Nature* **2005**, *438*, 197–200.
3. Zhang, Y.; Tan, Y.-W.; Stormer, H. L.; Kim, P. Experimental Observation of the Quantum Hall Effect and Berry's Phase in Graphene. *Nature* **2005**, *438*, 201–204.
4. Geim, A. K.; Novoselov, K. S. The Rise of Graphene. *Nat. Mater.* **2007**, *6*, 183–191.
5. Novoselov, K. S.; Falko, V. I.; Colombo, L.; Gellert, P. R.; Schwab, M. G.; Kim, K. A Roadmap for Graphene. *Nature* **2012**, *490*, 192–200.
6. Dean, J. J.; van Driel, H. M. Second Harmonic Generation from Graphene and Graphitic Films. *Appl. Phys. Lett.* **2009**, *95*, 261910.
7. Dean, J. J.; van Driel, H. M. Graphene and Few-Layer Graphite Probed by Second-Harmonic Generation: Theory and Experiment. *Phys. Rev. B* **2010**, *82*, 125411.
8. Mikhailov, S. A. Theory of the Giant Plasmon-Enhanced Second-Harmonic Generation in Graphene and Semiconductor Two-Dimensional Electron Systems. *Phys. Rev. B* **2011**, *84*, 045432.
9. Bykov, A. Y.; Murzina, T. V.; Rybin, M. G.; Obraztsova, E. D. Second Harmonic Generation in Multilayer Graphene Induced by Direct Electric Current. *Phys. Rev. B* **2012**, *85*, 121413.
10. Hong, S.-Y.; Dadap, J. I.; Petrone, N.; Yeh, P.-C.; Hone, J.; Osgood, R. M., Jr. Optical Third-Harmonic Generation in Graphene. *Phys. Rev. X* **2013**, *3*, 021014.
11. Gu, T.; Petrone, N.; McMillan, J. F.; van der Zande, A.; Yu, M.; Lo, G. Q.; Kwong, D. L.; Hone, J.; Wong, C. W. Regenerative Oscillation and Four-Wave Mixing in Graphene Optoelectronics. *Nat. Photonics* **2012**, *6*, 554–559.
12. Entin, M. V.; Magarill, L. I.; Shepelyansky, D. L. Theory of Resonant Photon Drag in Monolayer Graphene. *Phys. Rev. B* **2010**, *81*, 165441.
13. Karch, J.; Olbrich, P.; Schmalzbauer, M.; Zoth, C.; Brinsteiner, C.; Fehrenbacher, M.; Wurstbauer, U.; Glazov, M. M.; Tarasenko, S. A.; Ivchenko, E. L.; *et al.* Dynamic Hall Effect Driven by Circularly Polarized Light in a Graphene Layer. *Phys. Rev. Lett.* **2010**, *105*, 227402.
14. Jiang, C. Y.; Shalygin, V. A.; Panevin, V. Y.; Danilov, S. N.; Glazov, M. M.; Yakimova, R.; Lara-Avila, S.; Kubatkin, S.; Ganichev, S. D. Helicity-Dependent Photocurrents in Graphene Layers Excited by Midinfrared Radiation of a CO_2 Laser. *Phys. Rev. B* **2011**, *84*, 125429.
15. Glazov, M. M.; Ganichev, S. D. High Frequency Electric Field Induced Nonlinear Effects in Graphene. *Phys. Rep.* **2014**, *535*, 101–138.
16. Obraztsov, P. A.; Kaplas, T.; Garnov, S. V.; Kuwata-Gonokami, M.; Obraztsov, A. N.; Svirko, Y. P. All-Optical Control of

Ultrafast Photocurrents in Unbiased Graphene. *Sci. Rep.* **2014**, 4007.
17. Martinez, J. C.; Jalil, M. B. A.; Tan, S. G. Giant Faraday and Kerr Rotation with Strained Graphene. *Opt. Lett.* **2012**, *37*, 3237–3239.
18. Sun, D.; Divin, C.; Rioux, J.; Sipe, J. E.; Berger, C.; de Heer, W. A.; First, P. N.; Norris, T. B. Coherent Control of Ballistic Photocurrents in Multilayer Epitaxial Graphene Using Quantum Interference. *Nano Lett.* **2010**, *10*, 1293–1296.
19. Prechtel, L.; Song, L.; Schuh, D.; Ajayan, P.; Wegscheider, W.; Holleitner, A. W. Time-Resolved Ultrafast Photocurrents and Terahertz Generation in Freely Suspended Graphene. *Nat. Commun.* **2012**, *3*, 646.
20. Bonaccorso, F.; Sun, Z.; Hasan, T.; Ferrari, A. C. Graphene Photonics and Optoelectronics. *Nat. Photonics* **2010**, *4*, 611–622.
21. Bao, Q.; Loh, K. P. Graphene Photonics, Plasmonics, and Broadband Optoelectronic Devices. *ACS Nano* **2012**, *6*, 3677–3694.
22. Rana, F. Graphene Terahertz Plasmon Oscillators. *IEEE Trans. Nanotechnol.* **2008**, *7*, 91–99.
23. Ryzhii, V.; Ryzhii, M. Graphene Bilayer Field-Effect Phototransistor for Terahertz and Infrared Detection. *Phys. Rev. B* **2009**, *79*, 245311.
24. Vicarelli, L.; Vitiello, M. S.; Coquillat, D.; Lombardo, A.; Ferrari, A. C.; Knap, W.; Polini, M.; Pellegrini, V.; Tredicucci, A. Graphene Field-Effect Transistors as Room-Temperature Terahertz Detectors. *Nat. Mater.* **2012**, *11*, 865–871.
25. Boubanga-Tombet, S.; Chan, S.; Watanabe, T.; Satou, A.; Ryzhii, V.; Otsuji, T. Ultrafast Carrier Dynamics and Terahertz Emission in Optically Pumped Graphene at Room Temperature. *Phys. Rev. B* **2012**, *85*, 035443.
26. Newson, R. W.; Ménard, J.-M.; Sames, C.; Betz, M.; Driel, H. M. v. Coherently Controlled Ballistic Charge Currents Injected in Single-Walled Carbon Nanotubes and Graphite. *Nano Lett.* **2008**, *8*, 1586–1589.
27. Ramakrishnan, G.; Chakkittakandy, R.; Planken, P. C. M. Terahertz Generation from Graphite. *Opt. Express* **2009**, *17*, 16092–16099.
28. Dragoman, D.; Dragoman, M.; Hartnagel, H. Terahertz Generation Using a Resonant-Tunneling-like Configuration in Graphene. *J. Appl. Phys.* **2011**, *109*, 124307.
29. Karch, J.; Drexler, C.; Olbrich, P.; Fehrenbacher, M.; Hirmer, M.; Glazov, M. M.; Tarasenko, S. A.; Ivchenko, E. L.; Birkner, B.; Eroms; *et al.* Terahertz Radiation Driven Chiral Edge Currents in Graphene. *Phys. Rev. Lett.* **2011**, *107*, 276601.
30. Nagel, M.; Michalski, A.; Botzem, T.; Kurz, H. Near-Field Investigation of THz Surface-Wave Emission from Optically Excited Graphite Flakes. *Opt. Express* **2011**, *19*, 4667–4672.
31. Irfan, M.; Yim, J.-H.; Kim, C.; Wook Lee, S.; Jho, Y.-D. Phase Change in Terahertz Waves Emitted from Differently Doped Graphite: The Role of Carrier Drift. *Appl. Phys. Lett.* **2013**, *103*, 201108.
32. Gallot, G.; Grischkowsky, D. Electro-Optic Detection of Terahertz Radiation. *J. Opt. Soc. Am. B* **1999**, *16*, 1204–1212.
33. van der Valk, N. C. J.; Wenckebach, T.; Planken, P. C. M. Full Mathematical Description of Electro-Optic Detection in Optically Isotropic Crystals. *J. Opt. Soc. Am. B* **2004**, *21*, 622–631.
34. Sakai, K. *Terahertz Optoelectronics, Topics in Applied Physics*; Springer: Berlin, 2005.
35. Obraztsov, A. N.; Lyashenko, D. A.; Fang, S.; Baughman, R. H.; Obraztsov, P. A.; Garnov, S. V.; Svirko, Y. P. Photon Drag Effect in Carbon Nanotube Yarns. *Appl. Phys. Lett.* **2009**, *94*, 231112.
36. Mikheev, G. M.; Nasibulin, A. G.; Zonov, R. G.; Kaskela, A.; Kauppinen, E. I. Photon-Drag Effect in Single-Walled Carbon Nanotube Films. *Nano Lett.* **2011**, *12*, 77–83.
37. Obraztsov, P. A.; Mikheev, G. M.; Garnov, S. V.; Obraztsov, A. N.; Svirko, Y. P. Polarization-Sensitive Photoresponse of Nanographite. *Appl. Phys. Lett.* **2011**, *98*, 091903–3.
38. Echtermeyer, T. J.; Britnell, L.; Jasnos, P. K.; Lombardo, A.; Gorbachev, R. V.; Grigorenko, A. N.; Geim, A. K.; Ferrari, A. C.; Novoselov, K. S. Strong Plasmonic Enhancement of Photovoltage in Graphene. *Nat. Commun.* **2011**, *2*, 458.
39. Liu, Y.; Cheng, R.; Liao, L.; Zhou, H.; Bai, J.; Liu, G.; Liu, L.; Huang, Y.; Duan, X. Plasmon Resonance Enhanced Multicolour Photodetection by Graphene. *Nat. Commun.* **2011**, *2*, 579.
40. Cheon, S.; Kihm, K. D.; Park, J. S.; Lee, J. S.; Lee, B. J.; Kim, H.; Hong, B. H. How To Optically Count Graphene Layers. *Opt. Lett.* **2012**, *37*, 3765–3767.
41. Fang, Z.; Liu, Z.; Wang, Y.; Ajayan, P. M.; Nordlander, P.; Halas, N. J. Graphene-Antenna Sandwich Photodetector. *Nano Lett.* **2012**, *12*, 3808–3813.
42. Fang, Z.; Wang, Y.; Liu, Z.; Schlather, A.; Ajayan, P. M.; Koppens, F. H. L.; Nordlander, P.; Halas, N. J. Plasmon-Induced Doping of Graphene. *ACS Nano* **2012**, *6*, 10222–10228.
43. Kim, J.; Son, H.; Cho, D. J.; Geng, B.; Regan, W.; Shi, S.; Kim, K.; Zettl, A.; Shen, Y.-R.; Wang, F. Electrical Control of Optical Plasmon Resonance with Graphene. *Nano Lett.* **2012**, *12*, 5598–5602.
44. Lee, S. H.; Choi, M.; Kim, T.-T.; Lee, S.; Liu, M.; Yin, X.; Choi, H. K.; Lee, S. S.; Choi, C.-G.; Choi, S.-Y.; *et al.* Switching Terahertz Waves with Gate-Controlled Active Graphene Metamaterials. *Nat. Mater.* **2012**, *11*, 936–941.
45. Zhu, X.; Shi, L.; Schmidt, M. S.; Boisen, A.; Hansen, O.; Zi, J.; Xiao, S.; Mortensen, N. A. Enhanced Light Matter Interactions in Graphene-Covered Gold Nanovoid Arrays. *Nano Lett.* **2013**, *13*, 4690–4696.
46. Ramakrishnan, G.; Kumar, N.; Ramanandan, G. K. P.; Adam, A. J. L.; Hendrikx, R. W. A.; Planken, P. C. M. Plasmon-Enhanced Terahertz Emission from a Semiconductor/Metal Interface. *Appl. Phys. Lett.* **2014**, *104*, 071104.
47. Ramakrishnan, G.; Kumar, N.; Planken, P. C. M.; Tanaka, D.; Kajikawa, K. Surface Plasmon-Enhanced Terahertz Emission from A Hemicyanine Self-Assembled Monolayer. *Opt. Express* **2012**, *20*, 4067–4073.
48. Grosse, N. B.; Heckmann, J.; Woggon, U. Nonlinear Plasmon-Photon Interaction Resolved by k-Space Spectroscopy. *Phys. Rev. Lett.* **2012**, *108*, 136802.
49. Ramakrishnan, G.; Planken, P. C. M. Percolation-Enhanced Generation of Terahertz Pulses by Optical Rectification on Ultrathin Gold Films. *Opt. Lett.* **2011**, *36*, 2572–2574.